

Optimal Planning for Information Acquisition

Yonatan Silverman,¹ Lauren M. Miller,¹ Malcolm A. MacIver,^{1,2} and Todd D. Murphey,¹

Abstract—This paper presents an algorithm for active search where the goal is to calculate optimal trajectories for autonomous robots during data acquisition tasks. Formulating the problem as parameter estimation enables us to use Fisher information to create an explicit connection between robot dynamics and the informative regions of the search space. We use optimal control to automate design of trajectories that spend time in regions proportional to the probability of collecting informative data and use acquired data to update the probability closed-loop. Experimental and simulated results use a robotic electrosense platform to localize a feature in one-dimension. We demonstrate that this method is robust with respect to disturbances and initial conditions, and results in successful localization of the feature with a 100% experimental success rate and a 34% reduction in localization time compared to the next best tested controller.

I. INTRODUCTION

Acquiring information is a fundamental capability for sensing systems navigating unknown environments. Whether an autonomous vehicle traversing unfamiliar terrain or an animal looking for prey, collecting environmental data reduces to two central questions: where are the informative areas of the search domain, and given these areas how should the system make decisions about what actions to take? The interplay between these ideas drives the need for *active search*.

Active search should enable the sensing system to dynamically choose trajectories based on the current knowledge of the state, or lack thereof. Current active search algorithms attempt to minimize uncertainty or maximize information. However, because these metrics rely on optimizing expected observations, these methods are typically computationally expensive [1]. Using the South American weakly electric fish as a motivating biological example, we solve this problem more effectively than current techniques.

Figure 1a shows an electric fish, *Apteronotus albifrons*, and Fig. 1b demonstrates the fish’s unique sensing modality involving a self-generated electric field (reviews: [2], [3]). The fish has electroreceptors along the surface of its skin that are sensitive to changes in the electric field due to external objects. The electric fish demonstrates the importance of considering how the sensing modality effects the spatial distribution of sensory data. The voltage perturbation profile on the surface of the body (the electric image) is non-unique with respect to the distance of the object from the sensor, as

shown in Fig. 1c; it is not possible to uniquely determine object position from noiseless sensor measurements. The sensing range is also quite small—the fish has to be relatively close to an object to localize it. Additionally, the movement of the sensors involve the dynamics of the entire animal. Consideration of sensor dynamics and efficiency of the sensing trajectory when planning control for exploration is therefore especially important for the electric fish [4], and many other near field sensors, e.g. tactile sensors, ultra-shortwave sonar, and underwater image sensors (e.g. [5]).

We formulate an active search solution for general feature identification problems. This type of problem involves resolving the uncertainty of *environmental parameters* using noisy measurements. We do not take into account uncertainty in pose or process noise. Parameters are variables in the model of the system or environment. Examples include location, size, length, or conductivity of some feature which defines the map. In the example in Section III the parameter we estimate is the position of a submerged sphere.

The standard approach to search strategy in many active mapping problems involves defining a scalar metric over the entire search domain and then choosing a movement which minimizes that metric. Metrics such as entropy, variance, or A-, D-, E-optimality [1], [8]–[11] are often used. For example, one could represent the probabilistic belief as a distribution and calculate the control option that best minimizes the expected entropy. However, these technique can be computationally expensive, as an expected measurement has to be calculated for every update, and calculations increase exponentially with the number of parameters [1].

Rather than use a metric that requires calculation and propagation of the current belief of the uncertain parameter, we use Fisher information. Fisher information quantifies the ability of a random variable, in this case a measurement, to estimate an unknown parameter [12]. Fisher information is generally thought of only in parameter space, however, we extend the traditional understanding of Fisher information to the spatial domain, as the observation model depends on the spatial location of the sensor and parameter. As Section II-C will show, Fisher information predicts that the locations where the ratio of the derivative of the expected signal to the variance of the noise is high will give more salient data, and thus will be more useful for estimation.

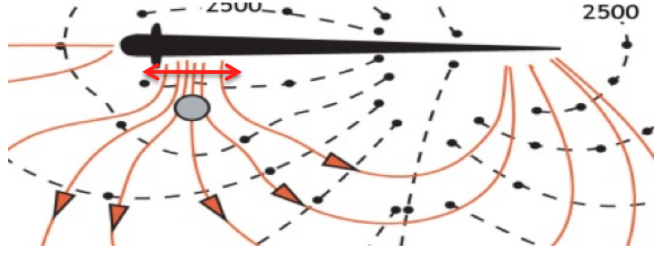
For our method, we express the Fisher information in terms of the measurement model (a function of sensor location and parameter value) and the parameter. Fisher information is generally defined with respect to an estimated or known value of the parameter. However, we define a probabilistic model over the parameter of interest (target

This work was supported by NSF grants IOB-0517683, CMMI-0941674, IIS 1018167, Office of Naval Research Small Business Technology Transfer grant N00014-09-M-0306 to M.A.M., and NIH grant T32 HD007418.

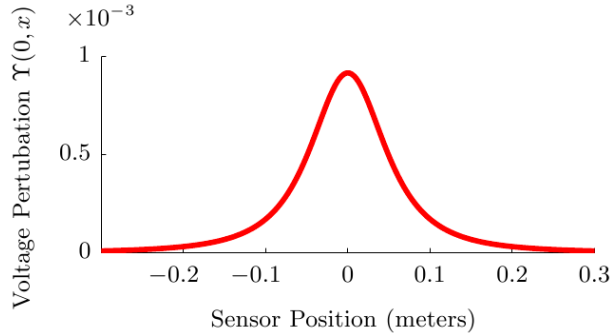
¹Department of Mechanical Engineering. ²Department of Biomedical Engineering. [1] and [2] at R.R. McCormick School of Engineering and Applied Science at Northwestern University, Evanston, Illinois, USA



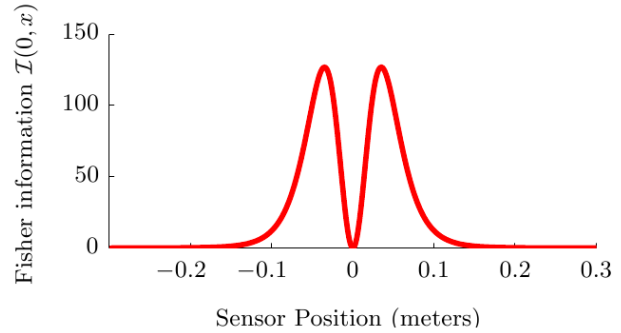
(a) The black ghost knifefish, *Apteronotus albifrons*. Photograph courtesy of Per Erik Svliland.



(b) A coronal view of the electric fish showing its self-generated electric field in 2D. The object (in gray) perturbs the electric field (black lines) and the isopotential lines (orange). Modified from [6], Fig. 2.



(c) A 1D model of the voltage perturbations along the red line in (b) using the equations presented in Chen et al. [7]. We assume a 1-inch diameter, non-conductive sphere, 7 cm away from the sensors.



(d) The Fisher information of the signal in (c). Maximally informative areas of the search domain are at $x = \pm 0.05$. Active search decisions should take this into account.

Fig. 1: Electric field perturbation and Fisher information for the electric fish.

location in the later example). We use a Bayesian model to update the probability based on collected measurements. In order to produce a continuous map of relevant and non-relevant search locations in the search domain, we take the expected value of the Fisher information with respect to the Bayesian-updated PDF of the parameter. We call this distribution the expected information distribution (EID). This formulation and expectation of the Fisher information allows us to connect the current knowledge of the parameter of interest to the informative regions of the search space, and ultimately to the sensor dynamics.

The next question is how to efficiently use the EID to plan and execute movement necessary for search. There are several factors which make this a nontrivial problem for both biological and robotic systems: 1) A sensor cannot move instantaneously to the areas where the EID is maximal and 2) there is a tradeoff between completeness of coverage and time and energy spent during exploration [13]. The simplest, commonly used, approach would be a greedy-type search strategy, where the sensor moves in the direction which locally maximizes the search metric [14]–[16], in our case the EID. This approach, while computationally simple, ignores sensor dynamics and convergence rates and accuracy often suffer due to local minima. We explicitly demonstrate this comparison in Section III.

We have therefore developed a search strategy which involves solving for a continuous, finite time horizon trajectory that takes into account the global structure of the EID. This approach involves two components: first, defining an objective function dependent on both control effort and the

concept of ergodicity relative to our EID [17], and second, using the objective function in infinite-dimensional trajectory optimization [18]. In this context, ergodicity is a way of relating the time-averaged behavior of the search trajectory to the EID. A maximally ergodic trajectory with respect to a spatial distribution is one for which the percentage of time spent in any region in space is equal to the measure of that region. This means that the sensor should spend more time collecting measurements in areas that are more likely to contain relevant data. Thus, we can calculate a continuous trajectory that optimally samples the EID that is guaranteed to be dynamically feasible, while balancing control effort.

In this work we consider a one-dimensional search domain. Our method, however, readily extends to higher dimensional search domains such as \mathbb{R}^2 or $SE(2)$ [19], as well as higher dimensional parameter spaces. Nevertheless, even in one dimension, we demonstrate significant improvement in performance over other approaches in Section III.

A. Motivation

The long term motivation of our work is three-fold. Our first motivation comes from understanding the science of biological electrolocation, in particular how this sensing modality is connected to motion during search. The sensing modality that we use in modeling and on our robot involves the same fundamental physics used by the electric fish, providing a valuable platform for comparison against biology and our methods involving Fisher information and ergodicity represent a first step towards a hypothesis of the basic concepts important in biological search. Our second motivation comes from an application-driven engineering

perspective. Electrosensing technology is highly adaptable for low velocity, highly motile vehicles operating in cluttered environments [10], and the distribution of sensors on the robot allows for omnidirectional sensing. Lastly, the main contribution of this paper is developing theory for robotic probabilistic search and estimation.

II. SEARCH ALGORITHM

A. Problem Definition and Notation

We developed an algorithm for an active search method with the goal of estimating an unknown environmental parameter, θ . We assume a single dimensional search domain $X \subset \mathbb{R}$. The algorithm assumes that we have a measurement model $v = \Upsilon(\theta, x) + \delta$, where v is the measurement and the sensor location, x , is deterministic. $\Upsilon(\cdot)$ is a function of sensor location and parameter and δ represents zero mean noise with variance σ^2 . The Fisher information is defined over x and θ , and is calculated offline.

An overview of our method is shown in Algorithm 1. The algorithm is written in terms of iterations of the search trajectory execution, not single measurements. The algorithm is initialized with an initial sensor position $x(0)$, voltage measurement $\mathbf{V}_0(0)$, and an initial distribution (uniform) representing the probability of the parameter value $p(\theta)$.

At each iteration, the PDF $p(\theta)$ is updated as defined in Section II-B, given the previously measured signal $\mathbf{V}_i(t)$ and trajectory $x_{i-1}(t)$. The expected value of the Fisher information, defined in Section II-C, is then taken with respect to the distribution $p(\theta)$, yielding the EID. The EID, is then used to calculate the optimally ergodic control for the subsequent search strategy of the sensor over sampling time T . This strategy is executed, collecting measurements. The algorithm terminates when the standard deviation of the PDF representing object location, $SD(\theta)$, is smaller than a chosen tolerance ϵ . Note that for noisy systems ϵ will be bounded away from zero.

Algorithm 1

- 1: Init. $p(\theta)$ to a uniform distribution
 - 2: Init. $x(0), \mathbf{V}_0(0), \Upsilon(\theta, x), \epsilon$
 - 3: Calculate the Fisher Information $I(\theta, x)$ using Eq. (6)
 - 4: **while** $SD(\theta) > \epsilon$ **do**
 - 5: Update $p_i(\theta)$ given $\mathbf{V}_i(t)$ according to Eq. (1)
 - 6: Calculated the EID using Eq. (7)
 - 7: Calculate optimally ergodic control $u_i(t)$
 - 8: Execute trajectory $x_i(t)$, measuring $\mathbf{V}_{i+1}(t)$
 - 9: $i=i+1$
 - 10: **end while**
-

B. Probabilistic Model and Bayesian Update

The PDF $p(\theta)$ at every iteration i of Algorithm 1 is updated using a Bayesian rule:

$$p(\theta|\mathbf{V}_i(t), x_i(t)) = \eta p(\mathbf{V}_i(t)|x_i(t), \theta)p(\theta), \quad (1)$$

where $p(\theta)$ is the probability calculated at the previous iteration, η is a normalization factor, and $p(\mathbf{V}_i(t)|x_i, \theta)$ is the innovation.

In order to calculate the innovation, we first find the difference between the expected value of the signal v calculated given the measurement model and the measured signal $\mathbf{V}_i(t_j)$ at every time step t_j along the trajectory. Defining

$$e_j(\theta) = \mathbf{V}_i(t_j) - \mathbb{E}[v|x_i(t_j), \theta] \quad (2)$$

as the error for each time step, we can calculate the probability of observing the measured signal dependent on the parameter value. The probability of observing v given the parameter θ is calculated as follows:

$$p(\mathbf{V}_i(t_j)|\theta, x_i(t_j)) = p(e_j(\theta)) \quad (3)$$

where the probability is defined by a zero mean distribution with variance σ^2 (zero error corresponds to the highest probability of a correct estimate). The innovation for the entire sampling trajectory at that iteration is the product of the probabilities for each sampling time t_j ,

$$p(\mathbf{V}_i(t)|\theta, x_i(t)) = \prod_{j=1}^T p(\mathbf{V}_i(t_j)|x_i(t_j), \theta). \quad (4)$$

C. Fisher Information

The formal definition of Fisher information using [12] for estimating a parameter θ is:

$$\mathcal{I}(\theta, x) = \int_v \left(\frac{\partial p(v|\theta)}{\partial \theta} \right)^2 \frac{1}{p(v|\theta)} dv. \quad (5)$$

When the objective is to estimate a parameter from a random variable $v \sim \mathcal{N}(\theta, \sigma^2)$, the Fisher information reduces to $\mathcal{I} = 1/\sigma^2$ [12]. However in our case, as our observation v is a random variable dependent on a function of the parameter θ , assuming Gaussian noise, the Fisher information for estimation of θ can be simplified to

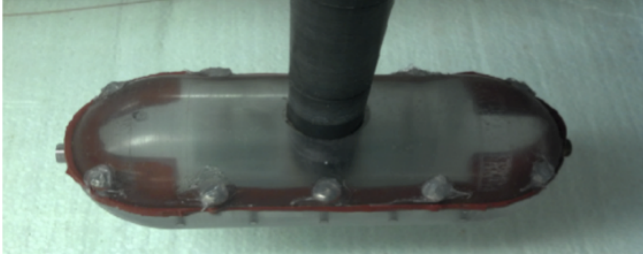
$$\mathcal{I}(\theta, x) = \left(\frac{\partial \Upsilon(\theta, x)}{\partial \theta} \cdot \frac{1}{\sigma} \right)^2. \quad (6)$$

$\partial \Upsilon(\cdot)/\partial \theta$ is the partial derivative of $\Upsilon(\cdot)$ with respect to the parameter. The Fisher information, $\mathcal{I}(\theta, x)$ can be thought of as the amount of information a measurement provides at location x for a given estimate of θ (based on the measurement model). For example, Fig 1d shows the Fisher information for the voltage perturbation transect in Fig 1c for a particular value of θ over the entire search domain. Since the value of θ is represented as a PDF as in Section II-B, we can take the expected value of $\mathcal{I}(\theta, x)$ with respect to $p(\theta)$ to determine the EID, $\Phi(x)$, over the search domain. The expected value is calculated as follows:

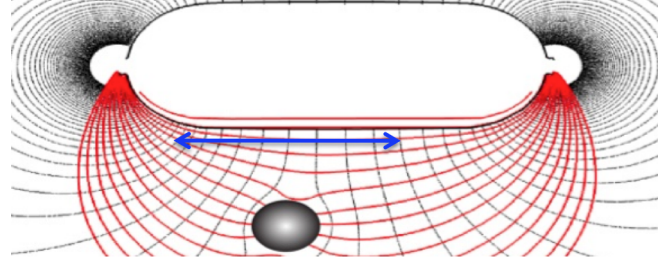
$$\Phi(x) = \int_{\theta} \mathcal{I}(\theta, x) p(\theta) d\theta. \quad (7)$$

D. Ergodic Optimal Control

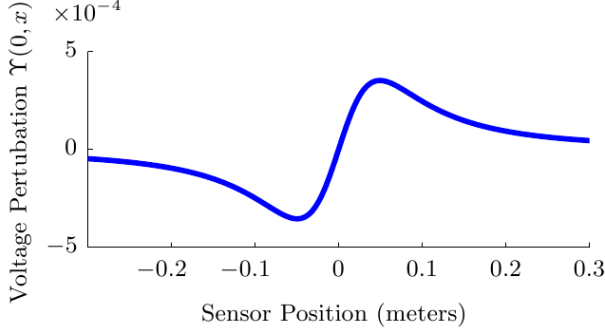
1) *Ergodic Metric*: Ergodicity is a statistical concept which relates the time-averaged behavior of a trajectory to a spatial distribution. The time-averaged behavior of a trajectory can be expressed as a distribution over the spatial domain by calculating the percentage of time the trajectory spends at each point x [17].



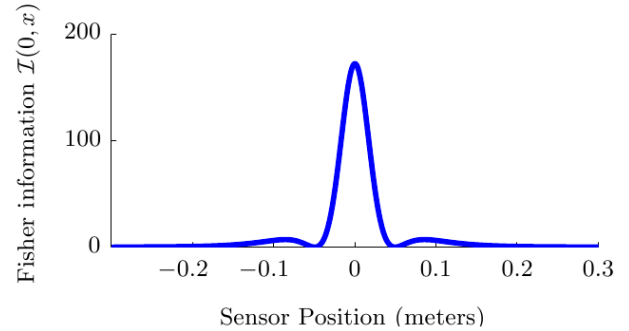
(a) An image of the SensorPod robot with excitation electrodes at either end and sensors that run axially down the pod.



(b) Top view of a model of the SensorPod showing its electric field. The object (in gray) perturbs the electric field lines (red) and the isopotential lines (black).



(c) A 1D model of the voltage perturbations along the blue line in (b) given a 1-inch diameter non conductive object located as shown



(d) The Fisher information of the signal in (c), highlighting that the globally maximally informative area of the search domain is at $x = 0$ with smaller maxima at $x = \pm 0.1$.

Fig. 2: Electric field perturbation and Fisher information for the SensorPod.

The metric used in our trajectory optimization will be the distance of the time-averaged trajectory from being ergodic with respect to the distribution $\Phi(x)$. This distance can be quantified by defining a norm on the Fourier coefficients of both distributions [17]. This norm is the sum of the weighted squared distance between the Fourier coefficients of the spatial distribution, ϕ_k , and those of the distribution representing the time-averaged trajectory, $c_k(x(t))$. The ergodic metric will be defined as $\mathcal{E}(x(t))$, as follows:

$$\mathcal{E}(x(t)) = \sum_{k=0}^K \Lambda_k |c_k(x(t)) - \phi_k|^2, \quad (8)$$

where K is the number of basis functions and Λ_k is a weighting factor [17]. When $\mathcal{E}(x(t)) = 0$, the statistics of the trajectory perfectly match those of the distribution $\Phi(x)$.

2) *Trajectory Optimization:* For a general, one dimensional system with dynamics $\dot{x}(t) = f(x(t), u(t))$ the goal is to solve for the continuous trajectory which minimizes an objective function based on both the ergodic metric and the control effort, defined as

$$J(x(t), u(t)) = Q\mathcal{E}(x(t)) + \int_0^T \frac{1}{2} R u(\tau)^2 d\tau, \quad (9)$$

where Q and R are scalar parameters defining the relative importance of minimizing ergodicity vs. control effort. Minimization of this objective function is accomplished using an extension of the projection-based trajectory optimization method presented in [20]. For details, see [18].

III. EXPERIMENTAL AND SIMULATED EXAMPLE

A. Model

The SensorPod (see Fig. 2) is a robotic electric fish that is inspired by the sensing capability of the electric fish in water. The SensorPod has two excitation electrodes that create an oscillating electric field, and 35 voltage sensors along the body. These sensors allow detection of voltage changes in all three spatial dimensions, and sample at 100 Hz.

We model the standard deviation of the measurement noise, σ , to be $100\mu V$, on the order of the noise level of the sensors in the SensorPod. The SensorPod is attached to 4-DOF gantry (x, y, z, Θ) which has a maximum speed of 2.2 m/s and can be accurately controlled to <1 mm. It is confined to a tank that is 1 by 2 meters and 1 meter deep. We assume a fixed angle Θ .

The task is to estimate the location α of a submerged object using the SensorPod. Chen et al. [7] describe the effects of spherical objects located in an electric field as

$$\Upsilon(\alpha, x) = \chi \frac{r^3 E(\alpha) \cdot (x - \alpha)}{|x - \alpha|^3}. \quad (10)$$

In this expression x is the location of the SensorPod, r the radius of the sphere, $E(\alpha)$ the electric field vector at the object's location, and χ a conductivity contrast factor. $\Upsilon(\alpha, x)$, assuming Gaussian noise, will serve as the measurement model for Algorithm 1. Note that the measurement model of the fish and SensorPod differ as the orientation of the generated electric fields are perpendicular, as shown in Figs. 1b and 2b. The formulation of the EID is applicable to any differentiable measurement model.

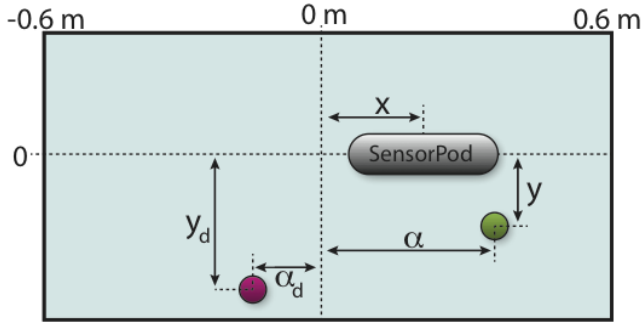


Fig. 3: Configuration for experimental and simulated trial. SensorPod, target and distractor object locations are measured from the center of the tank. Target object is in green, distractor in pink. y_d and y are fixed for all trials.

The design of the gantry system allows us to use a kinematic model of the SensorPod, i.e. the equations of motion are simply $\dot{x}(t) = u(t)$. For the present work, the kinematic model and one dimensional search space enable comparison with other search methods in Section IV. However, it should be noted that the method presented is applicable to dynamic, nonlinear systems as well.

B. Experimental Design

The SensorPod moves through the water along a straight line along the x axis as shown in Fig. 3. Two non-conductive spheres of 1-inch diameter are placed in the tank at fixed distances from the line of motion of the SensorPod. The closer sphere, green in Fig. 3, is the *target object*. The pink sphere is a *distractor object*. The target object was placed at a fixed distance of $y = 0.2$ meters from the SensorPod line of motion, and the distractor at $y_d = 0.25$ meters for all trials. Placing the distractor object further from the SensorPod line of motion has two effects; both the magnitude of the voltage trace and the rate of change are decreased. Because of this, the voltage signal from the distractor ball is similar but not identical to that of the target object. Figure 4 shows a simulated voltage profile measured across the search domain for both objects at the indicated positions along the x -axis. A minimum distance between objects was maintained, allowing us to model the two voltage signals as additive in the measurement model. In general, however, signals due to multiple objects are not additive [21].

We assess performance using failure rate and time to completion. We define failure as either exceeding 100 seconds before completion per trial, or converging to an object location greater than 1-cm from the correct value. This corresponds to an estimate more than twice the standard deviation used as our termination criterion.

We performed a Monte Carlo simulation for each control algorithm presented in section IV. We executed ten trials with the position of the target object at 11 equally spaced locations along the domain. For each of these 11 target locations, 10 locations for the distractor ball were randomly chosen, all at least 25 centimeters from target. 110 trials allowed significant separation of the results from different controllers while remaining tractable in simulation. In all trials, the

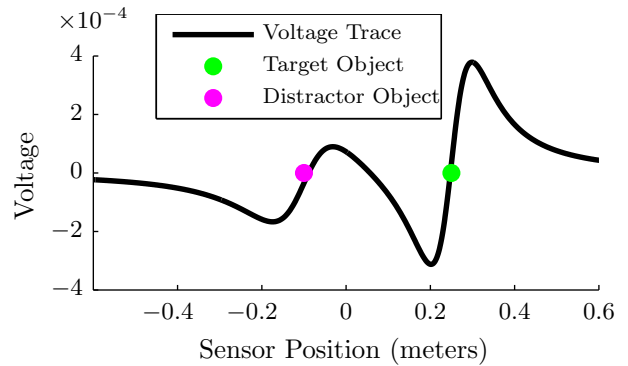


Fig. 4: The voltage perturbation for two objects in the domain. The target object has a peak voltage of ± 0.35 mV, and the distractor object has a peak voltage of ± 0.19 mV.

SensorPod position is initialized to $x, y = 0$. For each of the algorithms, measurements were made at 100 Hz along the trajectory. In simulation, Gaussian noise with standard deviation of $100\mu V$ was added to the measurement model.

For the simulated trials, our time horizon and update frequency were set to 1 second. In addition, we were able to update the probability function, $p(\alpha)$ after every measurement. In order to limit sloshing of the water in experiment, which negatively affects sensor readings, we had to limit the velocity of the SensorPod. Therefore, for the experimental trials we designed our ergodic trajectories with a time horizon of 8 seconds and set the weight on the control in the objective function (Eq. 9) accordingly. This gave us qualitatively similar trajectories to the simulated trials, as seen in Fig. 6, but with lower velocities.

1) *Comparison of Fisher information and minimum entropy controllers:* We use a single-step control algorithm to compare two versions of a minimum entropy metric to the metric we developed using Fisher information (not using trajectory optimization). The single-step control involves optimizing a metric to select a control action from a set of 100 predefined velocities over a fixed time horizon. We compare two versions of a standard minimum entropy metric and the metric using Fisher Information we developed.

For both minimum entropy methods, we use $\arg \max_u \int B(b, z, u)(x') \log B(b, z, u)(x') dx'$ [11] to define the objective function, where $B(b, z, u)$ is the belief after executing control u and observing z given the current belief b . We assess two different methods of calculation of the expected observation for this approach. For entropy controller #1 (EC1), the decrease in entropy after each potential control action is calculated using the expected observation given the maximum value of $p(\alpha)$. Entropy controller #2 (EC2) calculates the decrease in entropy for a given control action, where the expected observation is calculated for a weighted average of all possible object locations, weighted proportionally to $p(\alpha)$.

Finally, the Fisher information greedy controller (FG), calculates the integral over the EID for each control action. In all three cases, the metric is calculated for all potential control actions, and the action that maximizes the metric (minimal entropy or Fisher information) is chosen.

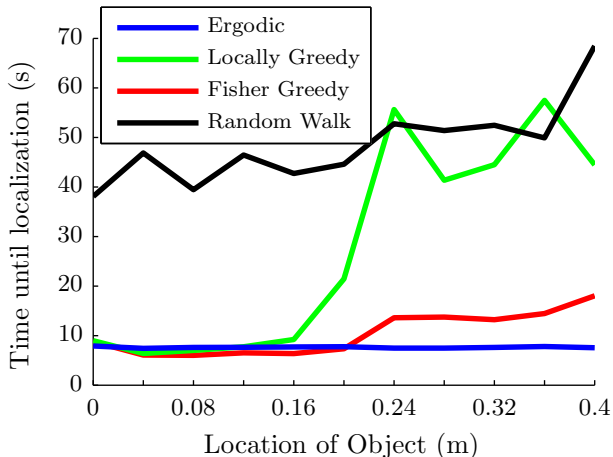


Fig. 5: Results for Monte Carlo simulation, where distractor location is randomly chosen for 11 fixed target locations. The ergodic controller has a 0% failure rate for all locations and the fastest average time to completion.

2) *Comparison of ergodic trajectory optimization and greedy controllers:* We evaluate the effectiveness of the approach in Algorithm 1 using the SensorPod in simulation and experimentally. In particular, we compare the performance of our ergodic algorithm (ER) to three versions of a standard greedy approach to solving this type of problem. All four are different ways of planning a search movement to sample the distribution $\Phi(x)$, allowing us to compare the use of a continuous ergodic search strategy to greedy approaches. The Fisher information greedy (FG) controller was the same one used in the previous claim. The discrete control action that maximizes the amount of Fisher information observed, defined by the EID, is chosen. The locally greedy controller (LG) takes a single step in the direction of the gradient of the EID at a fixed velocity of 4 cm/s at every update. The globally greedy controller (GG) calculates a trajectory to move to the location of the EID maximum. We also included a random walk (RW) controller that implements a step with a random velocity at every update.

IV. RESULTS AND DISCUSSION

Claim 1: Fisher information results in better performance than min-entropy: In table I, we compare the order of computation, the time required to perform all necessary calculations to select the optimal control action at each iteration, and success rate. These comparisons were only performed in simulation using Matlab.

| Description | EC1 | EC2 | FG |
|---------------------------------|-------------------|---------------------|-------------------|
| Order (n) | $\mathcal{O}(tn)$ | $\mathcal{O}(tn^2)$ | $\mathcal{O}(t)$ |
| Update ($\mu \pm \sigma$) (s) | 1.23 ± 0.08 | 1150 ± 17 | 0.084 ± 0.010 |
| Success (%) | 60% | 93% | 100% |

TABLE I: Data from 110 trials for each controller in simulation, where n is the size of the parameter space and t is the time per iteration.

Claim 1 demonstrates the benefit of using Fisher information over a more standard search metric such as minimization of entropy. EC1, which calculates the change in entropy considering the expected observation for the highest probability of the object location, was computationally efficient.

However, the algorithm had a success rate of only 60%, often failing due to local minima or resulting in incorrect localization of the distractor object, particularly for experimental configurations where the SensorPod was initialized closer to the distractor than the target (data not shown). The entropy controller that calculated the expected minimization of entropy based on the probability distribution (EC2) had a good success rate, however computation time averaged 20 minutes per iteration. Finally, the algorithm that chose control actions which maximized the Fisher information over the EID (FG) was always successful and able to update the trajectory in under a tenth of a second.

Claim 2: Ergodic trajectory optimization outperforms other controllers using Fisher Information: The results in simulation and experiment for success rate and average time until completion, for successful trials only, are summarized in Fig. 5 and Table II. Figure 6 shows the closed-loop optimally ergodic trajectory algorithm with respect to the EID using the Fisher information metric. The EID is shown as a density in blue. A single trial is shown for both the simulated and experimental system. Table II and Fig. 5 show that both

| Description | ER | GG | LG | FG | RW |
|------------------|------|------|------|------|------|
| Exp. Success (%) | 100% | 60% | 50% | – | – |
| Exp. Time (s) | 15.2 | 32.2 | 41.0 | – | – |
| Sim. Success (%) | 100% | 71% | 66% | 100% | 99% |
| Sim. Time (s) | 7.6 | 16.0 | 17.6 | 10.6 | 48.1 |

TABLE II: Data from experiment and simulation

in simulations and experiments, the ergodic controller with Fisher information always successfully located the target object, and on average more quickly than the greedy algorithms and random walk.

When the target position was close to the SensorPod initial position ($\alpha < 0.1$ m), the algorithms perform comparably. However for the greedy algorithms, the further the target was from the initial starting point of the SensorPod, the more likely the method was to fail or spend a large amount of time in regions of local minima caused by the presence of the distractor object. The ergodic controller, on the other hand, localized the ball in essentially constant time and with 0% failure rate. Our results demonstrate that the main benefits of the ergodic trajectory optimization algorithm are that the search strategy is essentially insensitive to the initial conditions (i.e. whether or not the sensor happens to start out closer to the distractor or target object) and robust in the presence of disturbances.

Simulation and experimental results for time to completion are dissimilar because of velocity constraints; experimental trials mandated slower trajectories, updated every 8 seconds. However, both of the ergodic trajectories were able to complete the task with 100 % success rate. These experiments demonstrate the benefit of performing a continuous trajectory optimization using the ergodic metric on the Fisher information: the Fisher information allows us to define a measure over the entire search domain which predicts where the most valuable measurements can be found, and the

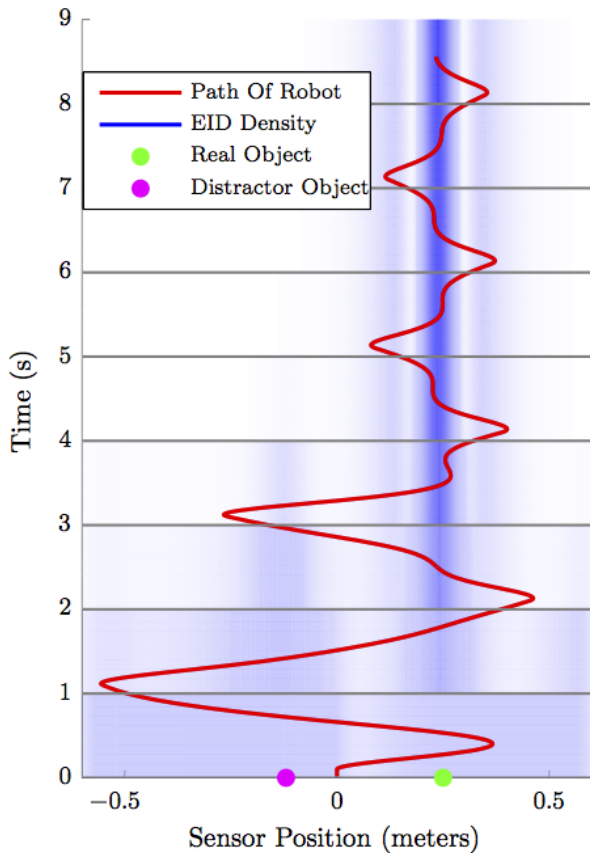


Fig. 6: An example of closed-loop optimally ergodic search in simulation is shown. The EID is shown as a density plot. The ergodic trajectory initially sweeps a large area given the nearly uniform EID, exploring progressively less of the domain as the uncertainty decreases.

ergodic trajectory optimization allows us to take advantage of this global distribution, calculating a trajectory that samples proportionally to the amount of Fisher information expected in a given region.

V. FUTURE WORK

We are developing an implementation of this algorithm in higher dimensional search domains. While not an issue in the 1D search domain, electrosense is orientation dependent. The search algorithm will therefore be implemented in $SE(2)$ and $SE(3)$ for more complex robot dynamics [22]. We also plan to generalize the method to allow calculation of optimal trajectories for multiple robots. Since Fisher information is additive [12], we are also able to consider multiple parameters by taking the expected value with respect to multiple probability functions. In addition, a parameter of interest does not have to be the location of an object within the search domain; all that is required is a differentiable observation model that relates the parameter of interest to the search domain. For example, future work will involve estimating the location of a sphere in two dimensions as well

as the radius of the sphere. Finally, we plan to extend the ergodic control strategy to include time horizon and sampling time optimization, allowing us to optimize the way in which we formulate the receding horizon control problem, further reducing localization time.

REFERENCES

- [1] C. Leung, S. Huang, N. Kwok, and G. Dissanayake, "Planning under uncertainty using model predictive control for information gathering," *Robotics and Autonomous Systems*, 2006.
- [2] R. W. Turner, L. Maler, and M. Burrows, "Special issue on electroreception and electrocommunication," *J. Exp. Biol.*, vol. 202, no. 10, pp. 1167–1458, 1999.
- [3] M. E. Nelson and M. A. MacIver, "Sensory acquisition in active sensing systems," *J. Comp. Physiol. A*, vol. 192, no. 6, pp. 573–586, 2006.
- [4] M. A. MacIver, A. A. Shirgaonkar, and N. A. Patankar, "Energy-information trade-offs between movement and sensing," *PLoS Computational Biology*, 2010.
- [5] S. Cowen, S. Briest, and J. Dombrowski, "Underwater docking of autonomous undersea vehicles using optical terminal guidance," in *MTS/IEEE OCEANS Conf.*, vol. 2, Oct 1997, pp. 1143–1147.
- [6] E. I. Knudsen, "Spatial aspects of the electric fields generated by weakly electric fish," *J. Comp. Physiol.*, vol. 99, no. 2, pp. 103–118, 1975.
- [7] L. Chen, J. H. House, R. Krahe, and M. E. Nelson, "Modeling signal and background components of electrosensory scenes," *J. Comp. Physiol. A*, vol. 191, pp. 331–345, 2005.
- [8] D. Fox, W. Burgard, and S. Thrun, "Active markov localization for mobile robots," *Robotics and Autonomous Systems*, vol. 25, no. 3-4, pp. 195–207, 1998.
- [9] R. Sim and N. Roy, "Global α -optimal robot exploration in slam," in *IEEE International Conference on Robotics and Automation*, 2005.
- [10] J. R. Solberg, K. M. Lynch, and M. A. MacIver, "Active electrolocation for underwater target localization," *International Journal of Robotics Research*, vol. 27, no. 5, pp. 529–548, 2008.
- [11] S. Thrun, W. Burgard, and D. Fox, *Probabilistic Robotics*. Cambridge, Mass: The MIT Press, 2005.
- [12] R. B. Frieden, *Science from Fisher Information A Unification*. Cambridge University Press, 2004.
- [13] J. G. March, "Exploration and exploitation in organizational learning," *Organization Science*, vol. 2, no. 1, February 1991.
- [14] Y. F. Li and Z. G. Liu, "Information entropy based viewpoint planning for 3-d object reconstruction," *IEEE Transactions on Robotics*, vol. 21, no. 3, pp. 324–327, 2005.
- [15] P. Whaite and F. P. Ferrie, "Autonomous exploration: driven by uncertainty," *IEEE Transactions on Pattern Analysis and Machine Intelligence*, vol. 19, no. 3, pp. 193–205, 1997.
- [16] H. J. S. Feder, J. J. Leonard, and C. M. Smith, "Adaptive mobile robot navigation and mapping," *International Journal of Robotics Research*, vol. 18, no. 7, pp. 650–668, 1999.
- [17] G. Mathew and I. Mezic, "Metrics for ergodicity and design of ergodic dynamics for multi-agent systems," *Physica D-nonlinear Phenomena*, vol. 240, no. 4-5, pp. 432–442, Feb 2011.
- [18] L. M. Miller and T. D. Murphey, "Trajectory optimization for continuous ergodic exploration," in *American Controls Conf. (ACC)*, 2013.
- [19] T. D. M. Lauren M. Miller, "Trajectory optimization for continuous ergodic exploration on the motion group $se(2)$," in *IEEE International Conference on Decision and Control*, submitted.
- [20] J. Hauser, "A projection operator approach to the optim. of trajectory functionals," in *IFAC world congress*, vol. 4, 2002, pp. 3428–3434.
- [21] D. Rother, A. Migliaro, R. Canetti, L. Gomez, A. Caputi, and R. Budelli, "Electric images of two low resistance objects in weakly electric fish," *Biosystems*, vol. 71, pp. 171–179, 2003.
- [22] N. Mahmoudian, C. Woolsey, and J. Geisbert, "Approximate analytical turning conditions for underwater gliders: Implications for motion control and path planning," in *IEEE Journal of Oceanic Engineering*, vol. 35, no. 1, 2010.